[zipi.endm67.cbn9710]cbn9710.tex CBN 97-10
5/2/1997

3-D Numerical Code for Field Calculations of Superconductive Magnets

Z. Greenwald
Laboratory of Nuclear Studies, Cornell University, Ithaca, NY 14853

May 2, 1997

Introduction

Phase III upgrade of CESR includes super conducting magnets without iron. The magnets are built from super conducting wire loops wrapped on a pipe. Because of the high currents involved in super conducting magnets, the distortion of the magnetic fields at the rounded ends may not be negligible and should be calculated. The gradual decrease in the magnetic field at the edges causes higher order multipoles, and the parasitic magnetic field in the z direction at the edges might cause coupling. In order to study these problems a 3-D numerical code was developed. The code BST.c calculates the spatial magnetic fields generated by a wire carrying current. In particular, it calculates fields of wire loops wrapped on a pipe. The arrangement and dimensions of the loops can be easily modified to create dipoles, quadruples, skew magnets etc.. It has been used to calculate the magnetic fields inside and outside the magnets. The higher order multipoles are obtained by a Fourier transformation of the field. It calculates local fields errors due to possible manufacturing imperfections. It also calculates the particle trajectories inside the magnet in order to investigate possible coupling between the horizontal and the vertical motion due to B_z at the ends. The effective magnet length was calculated by numerical integration over the whole magnet.

1 *Current Loops Characterization - Quadrupole*

An example of the magnetic fields of a quadrupole made out of four loops of wire ribbon is shown in Figure 1. The ribbon loops are wrapped on the pipe touching each other and creating four poles. (Current flows in opposite direction in each loop). The arcs of the loops in this example are circular. The magnet is illustrated in cylindrical coordinates with the z axis along the center of the pipe. When looking at the cross section $Z - Z_1$ of a pipe with four loops winding for a quadrupole as shown in Figure 2, there are four conducting sections, each of them is composed of two adjacent loops with width d (30° in a quadrupole). Each one of the eight sections d is composed of n_{wire} wires. The current **I** in each wire is described by the following function:

$$\mathbf{I} = (e_1, e_2, Ang[i], sign[i], I_c[i]) \tag{1}$$

where $i = 1, 2, 3, ...8$

The angle from the line $\theta = 0$ to the center of each one of the four loops is given by $Ang[i]$:

$$Ang[i] = \{45, 45, 135, 135, 225, 225, 315, 315\} \tag{2}$$

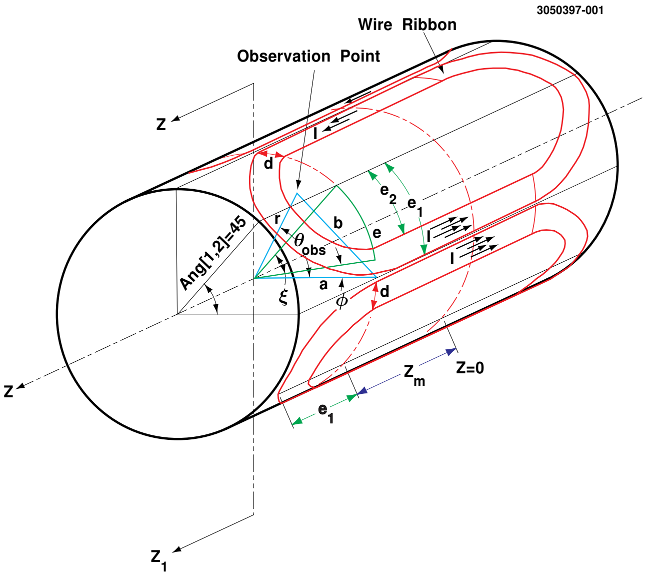

Figure 1: A Quadrupole magnet made out of four loops of wire ribbons

The location of the conductive wires in section i relative to $Ang[i]$ is indicated by the vector $sign[i]$:

$$sign[i] = \{-1, 1, -1, 1, -1, 1, -1, 1\} \tag{3}$$

where -1 indicates that the wires in the i section are below the center of the loop and $+1$ indicates that the wires in section i are above the center of the loop.

The direction of the current flow in each section i is given by:

$$I_c[i] = \{-1, 1, 1, -1, -1, 1, 1, -1\} \tag{4}$$

ξ is the angle measured from the center of the loop (at Ang[i=1]) to a wire in section $i = 1$

$$\xi = \begin{cases} \frac{e}{2\pi a} \cdot 360. & \text{along the stright conductor } |z| \leq z_m \\ \frac{e \sin\left(\arccos\left(\frac{z - z_m}{e}\right)\right)}{2\pi a} \cdot 360. & \text{along the arc } |z| > z_m \end{cases}$$

where z_m is the length of half the straight section.

In the straight section $|z| < z_m$, e is the part of the circumference from the loop center Ang[i=1] to any conducting wire in section $i = 1$. e_1 is the distance on the pipe circumference from the center Ang[i=1] to the outermost wire in section $i = 1$ and e_2 is the distance to the innermost wire in section $i = 1$

$$e_1 = \frac{2.\pi a}{8.} \tag{5}$$

$$e_2 = e_1 - d. \tag{6}$$

where a is the pipe radius.

ξ_1 is the angle to the outermost wire in section $i = 1$.

$$\xi_1 = \xi(e = e_1) \tag{7}$$

ξ_2 is the angle to the innermost wire in section$i = 1$.

$$\xi_2 = \xi(e = e_2) \tag{8}$$

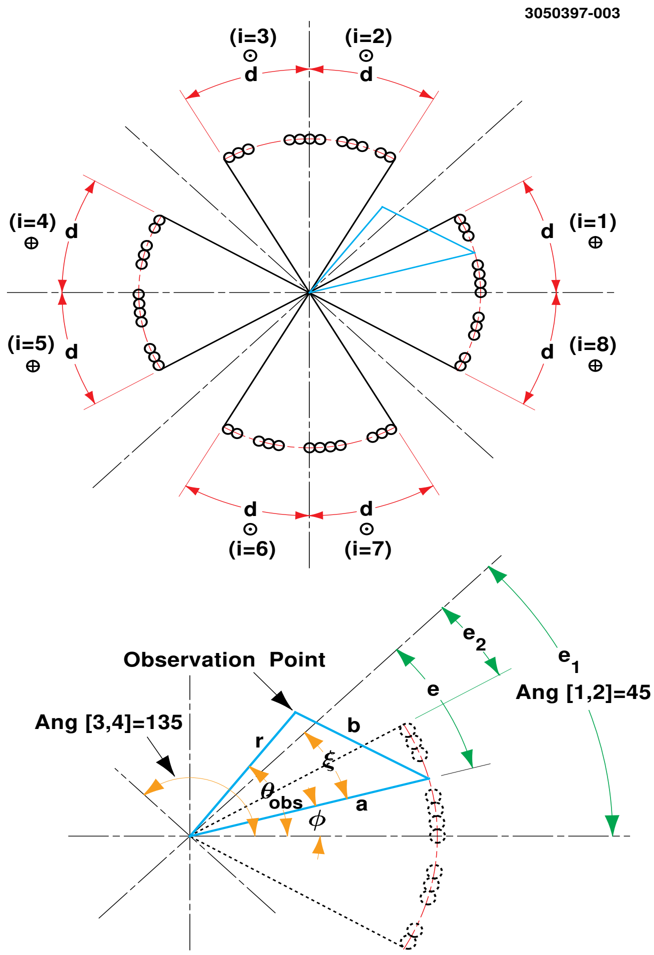

Figure 2: Coss section of a quadrupole magnet

i	Wire Locations	Current
1	$45 - \xi_1 \leq \Phi < 45 - \xi_2$	-I
2	$45 + \xi_2 \leq \Phi < 45 + \xi_1$	I
3	$135 - \xi_1 \leq \Phi < 135 - \xi_2$	I
4	$135 + \xi_2 \leq \Phi < 135 + \xi_1$	-I
5	$225 - \xi_1 \leq \Phi < 225 - \xi_2$	-I
6	$225 + \xi_2 \leq \Phi < 225 + \xi_1$	I
7	$315 - \xi_1 \leq \Phi < 315 - \xi_2$	I
8	$315 + \xi_2 \leq \Phi < 315 + \xi_1$	-I

Table 1: Eight spatial location of the wires in a quadrupole

he angle, Φ, is measured in each $(r - \theta)$ plane from $\theta = 0.$ to a conductive wire in any section.

$$\Phi = Ang[i] + \xi \cdot sign[i] \tag{9}$$

Its range of changes is summarized in Table 1 for $|z| < z_m$.

2 *Magnetic Field Calculations*

The magnetic field at each spatial point (r, θ_{obs}, z) is calculated using Biot-Savart law:

$$\mathbf{B}(r, \theta_{obs}, z) = \frac{\mu_o}{4\pi} \int \frac{\mathbf{I} \times \hat{\mathbf{R}}}{\mathbf{R^2}} dl_w \tag{10}$$

$\mathbf{B}$ is the magnetic field, dl_w is an element of length along the wire, $\mathbf{R}$ is the distance from the observation point (r, θ_{obs}, z) to dl_w and it changes as we integrate along the loop. The integration is done along each wire in all the sections $i = 1, 2..8$ along each half of a loop and the vectorial contributions seen at (r, θ_{obs}, z) from all the sections are summed up. Each section i has its own current sign $I_c[i]$ and it extends from $-(e + z_m)$ to $(e + z_m)$ (in a circular ends), where $|z| \leq z_m$ is the range of the straight section of the conductor. In order to calculate the Biot Savart integral all vectors were expressed in cylindrical coordinates. R_r, R_θ and R_z are the projections of the unit vector $\hat{\mathbf{R}}$ (in the direction of $\mathbf{R}$) on the direction r, θ and z correspondingly, see Appendix 1.

$$\hat{\mathbf{R}} = R_r \hat{r} + R_\theta \hat{\theta} + R_z \hat{z}. \tag{11}$$

Along the the straight conductors of the magnet, for $|z| \leq z_m$, the current $\mathbf{I}$ flows in the z direction only. While at the ends, where the wires are curved, the current has also a component I_l tangential to the pipe surface. See Appendix 2. I_l is further being projected on r and θ.

$$\mathbf{I} = \begin{cases} I_z \hat{z} & \textbf{along the stright conductor } |z| \leq z_m \\ I_r \hat{r} + I_{theta} \hat{\theta} + I_z \hat{z} & \textbf{along the arc } |z| > z_m \end{cases}$$

By substituting the vectors $\mathbf{I}$, $\hat{\mathbf{R}}$ and $\mathbf{R}$ in Equation 8 and approximating the integration by summation, we can get the magnetic field components. In a quadrupole, for example, there are $i = 8$ sections of half loops as seen in the cross section of the magnet (Figure 2). Each of the sections i has n_{wire} wires covering a width d. Thus the wires are separated from each other by $\Delta e = d/n_{wire}$ which determine the summation increments of e.

$$B_r = \sum_{i=1}^{8} \sum_{e=e1}^{e1-d} \sum_{z=-(z_m+e_1)}^{z_m+e_1} \frac{\mu_o}{4\pi} I_c[i] \frac{(I_\theta R_z - I_z R_\theta) \cdot dl_w}{R^2} \tag{12}$$

$$B_\theta = \sum_{i=1}^{8} \sum_{e=e1}^{e1-d} \sum_{z=-(z_m+e_1)}^{z_m+e_1} \frac{\mu_o}{4\pi} I_c[i] \frac{(I_z R_r - I_r R_z) \cdot dl_w}{R^2} \tag{13}$$

$$B_z = \sum_{i=1}^{8} \sum_{e=e1}^{e1-d} \sum_{z=-(z_m+e_1)}^{z_m+e_1} \frac{\mu_o}{4\pi} I_c[i] \frac{(I_r R_\theta - I_\theta R_r) \cdot dl_w}{R^2} \tag{14}$$

If we numerically integrate in equal steps of Δz along each wire in the magnet $dl_w = \Delta z$ along the straight conductor, while at the arc dl_w is different for each Δz. . See Appendix 3.

The accuracy of the calculation at each observation point (r, θ_{obs}, z) is determined by the steps size Δz which can be made smaller at particular areas of interest. The magnetic field in any direction is calculated by moving the observation point in this direction.

3 *Conclusions*

In order to check the results the numerically calculated fields were plugged in the equations of $\bigtriangledown \cdot \mathbf{B}$ and $\bigtriangledown \times \mathbf{B}$. Both expressions were approaching zero. Some examples of field calculation inside and outside of a quadrupole and a dipole with elliptical loop ends and equal perimeter in all layers can be seen in CBN 96-09. Also calculated there are the fields due to possible alignment errors.

4 *Appendix 1*

5 *Calculation of the cylindrical projections of the vector R*

R is the vector connecting a spot on the conducting wire with the observation point (r, θ_{obs}, z). see Figure 3.

5.1 Projection of the Unit Vector $\hat{\mathbf{R}}$ on the Vector r

$$b^2 = a^2 + r^2 - 2ar \cdot \cos(\theta_{obs} - \Phi) \tag{15}$$

$$R = \frac{b}{\cos\left(\arctan\left(\frac{z - z_{obs}}{b}\right)\right)} \tag{16}$$

$$k^2 = R^2 + r^2 - 2Rr \cdot \cos(q) \tag{17}$$

$$R_r = \cos(q) = \frac{R^2 + r^2 - k^2}{2Rr} \tag{18}$$

5.2 Projection of the Unit Vector $\hat{\mathbf{R}}$ on z

$$b^2 = R^2 + (z - z_{obs})^2 - 2R(z - z_{obs}) \cdot \cos(w) \tag{19}$$

$$R_z = \cos(w) = \frac{R^2 + (z - z_{obs})^2 - b^2}{2R(z - z_{obs})} \tag{20}$$

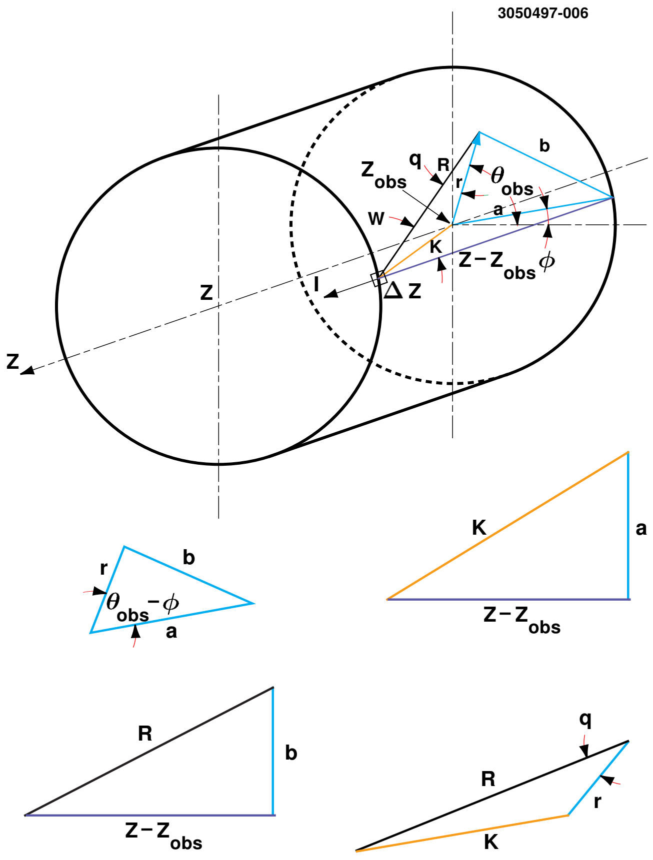

Figure 3: A slice of a pipe with a conducting wire

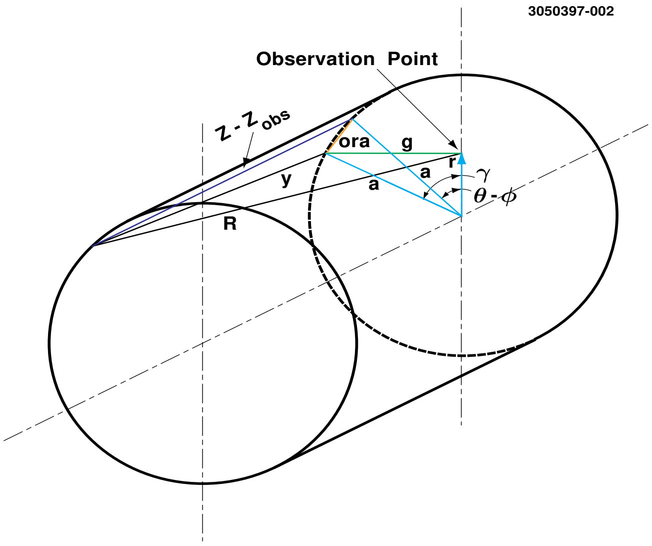

Figure 4: A cross section of a pipe

5.3 Projection of Unit Vector $\hat{\mathbf{R}}$ on θ

If we draw a line perpendicular to r from the observation point to the pipe circumference, see figure 4, then:

$$\gamma = \arccos\left(\frac{r}{a}\right) \tag{21}$$

$$g = \tan\left(\arccos\left(\frac{r}{a}\right)\right) \tag{22}$$

$$ora = 2a\sin\left(\frac{\theta - \Phi - \gamma}{2.}\right) \tag{23}$$

$$y = \frac{ora}{\cos\left(\arctan\left(\frac{z - z_{obs}}{ora}\right)\right)} \tag{24}$$

R_θ is the projection of the unit vector $\hat{\mathbf{R}}$ on g.

$$R_\theta = \frac{R^2 + g^2 - y^2}{2gR} \tag{25}$$

6 *Appendix 2*

7 *Calculation of the Current Components in Cylindrical Coordinates.*

Along the straight lines of the quadrupole the current flows in the z direction. At the ends the wire bends to create the loop. The current is no longer in the z direction. It can be decompose to I_z and I_l, where I_l is the component of the current which is tangential to the pipe circumference at the wire. (see Figure 5)

7.1 Projection of I on z and on the tangent to the pipe ,l.

$e_1 \leq e < e_2$

$$l = e \cdot \sin(\alpha) = e \cdot \sin\left(\arccos\left(\frac{z - z_m}{e}\right)\right) \tag{26}$$

The z and l components of the current for a circular end loop are:

$$I_z = I \cdot \sin\left(\arccos\left(\frac{z - z_m}{e}\right)\right) \tag{27}$$

$$I_l = I \cdot \cos\left(\arccos\left(\frac{z - z_m}{e}\right)\right) \tag{28}$$

This current need to be projected on r and θ.

7.2 Projection of I_l on r and θ

$$I_{lr} = I_l \cdot \sin(\theta - \Phi) \tag{29}$$

$$I_{l\theta} = I_l \cdot \cos(\theta - \Phi) \tag{30}$$

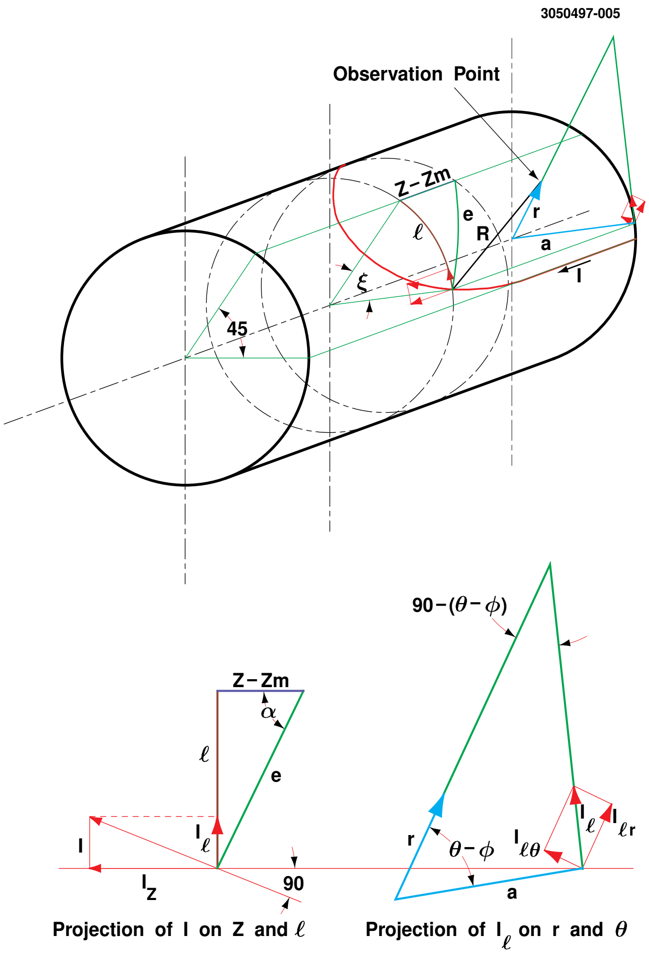

Figure 5: Eliptical End of the Wire Loop

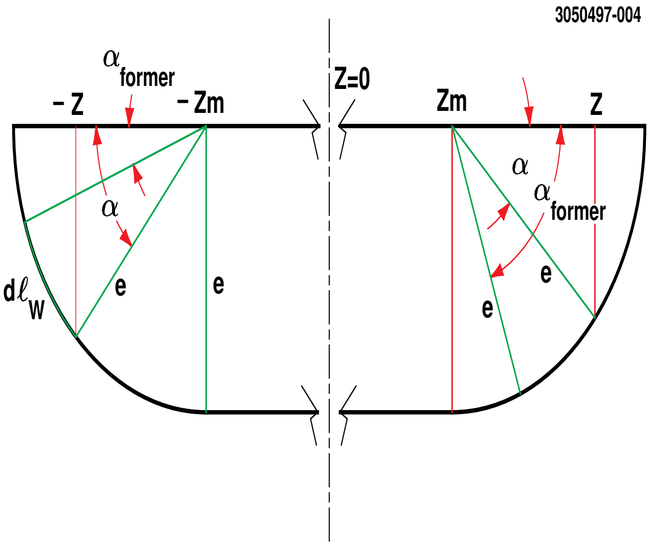

Figure 6: A Slice of the Magnet at the End of the Wire Loop

8 *Appendix 3*

9 *Calculation of dl_w at the arcs*

The numerical integration is done in steps of Δz. Thus dl_w equals Δz in the straight part, but has various length along the arcs. See Figure 6. For a circular end loop $z_m < |z| \leq z_m + e$

$$\alpha = \arccos\left(\frac{|z| - z_m}{e}\right) \tag{31}$$

For each step, Δz, dl_w in the arc is given by:

$$dl_w = \frac{2.\pi e|(\alpha - \alpha_{former})|}{360.} \tag{32}$$

Calculating dl_w, starting from negative z, the initial value of α, α_{former}, are zero. For the next step Δz the value of α_{former} is set to the value of the last α

$$\alpha_{former} = \alpha \tag{33}$$

The absolute values were put to make the routine valid for the arcs on both sides of the loop. Note, when the integration is done over the arc on the $(z > 0)$ side, the initial value of α_{former} should be $\pi/2$ which is the last value stored on the left side calculations $(z < 0.)$.

Acknowledgment

We would like to thank Gerry Dugan for very helpful discussions.